Copyright by the American Physical Society. Schulz, K. H.; Cox, D. F., "Photoemission and low-energy-electron-diffraction study of clean and oxygen-dosed Cu2O (111) and (100) surfaces," Phys. Rev. B 43, 1610 DOI: http://dx.doi.org/10.1103/PhysRevB.43.1610

PHYSICAL REVIEW B VOLUME 43, NUMBER 2 15 JANUARY 1991-I

Photoemission and low-energy-electron-diffraction study of clean and oxygen-dosed Cu_2O (111) and (100) surfaces

Kirk H. Schulz and David F. Cox*
Department of Chemical Engineering, Virginia Polytechnic Institute and State University, Blacksburg, Virginia 24061
(Received 5 July 1990)

The geometric and electronic structure of clean and oxygen-dosed Cu_2O single-crystal surfaces was studied with x-ray and ultraviolet photoelectron (UPS) spectroscopies and low-energy electron diffraction. The nonpolar (111) surface can be prepared in a nearly stoichiometric (1×1) form by ion bombardment and annealing in vacuum. Oxygen adsorbs molecularly on the stoichiometric (111) surface at 300 K, but adsorbs dissociatively on a defective (111) surface prepared by ion bombardment. For the polar $Cu_2O(100)$ face it was possible to prepare a reconstructed, Cu-terminated surface with a $(3\sqrt{2}\times\sqrt{2})R45°$ periodicity by ion bombardment and annealing in vacuum. Preparation of an unreconstructed, (1×1), O-terminated (100) surface was possible by large (10^9-L) oxygen exposures. UPS investigations of the O-terminated (100) surface suggest a mixture of incorporated (i.e., lattice) oxygen and adsorbed atomic oxygen (i.e., adatoms) in the terminating layer. The annealing behavior of the $Cu_2O(100)$ surface was history dependent. Early in the sample history, bulk lattice oxygen diffused to the surface at temperatures above 800 K giving domains of $(\sqrt{2}\times\sqrt{2})R45°$ periodicity associated with half a terminating layer of oxygen atoms. After repeated ion bombardment and annealing cycles, heating above 800 K gave only a Cu-terminated surface, apparently because of a depletion of bulk lattice oxygen.

I. INTRODUCTION

The surface properties of the oxygen-copper system have been investigated extensively for over 25 years in an effort to understand the structure and electronic properties of both adsorbed and incorporated (oxide) oxygen (Ref. 1, and references therein). Recently, there has been a renewed interest in the electronic properties of copper oxides because of the advances in high-T_c copper oxide superconductors. Cuprous oxide, Cu_2O, is a p-type semiconductor with the cuprate structure ($Pn3$). From a structural viewpoint, Cu_2O is interesting because it possesses unusual linear O—Cu—O bonds.[2] From an electronic viewpoint, bulk Cu_2O has been investigated because of interest in its Wannier-exciton spectrum.[3] There are no previously reported photoemission or low-energy electron-diffraction (LEED) studies for Cu_2O single-crystal surfaces.

Herion *et al.*[4] studied the effects of electron irradiation on the $Cu_2O(111)$ surface, and noted that no degradation occurred during electron-beam exposures in Auger-electron spectroscopy (AES). They observed no preferential removal of oxygen during ion bombardment of the $Cu_2O(111)$ surface, and suggested that clean, stoichiometric $Cu_2O(111)$ surfaces could be prepared by ion bombardment and annealing.[4] Panzner *et al.*[5] examined the effect of Ar-ion bombardment on Cu_2O layers prepared by oxidation of a copper single crystal. They found no detectable reduction of the surface for 3-keV Ar-ion sputtering, but some Cu metal was observed following bombardment with 5-keV Ar ions.[5]

Several groups have studied the conductivity of Cu_2O single crystals as a function of both annealing temperature and oxygen partial pressure.[6–8] A study of $Cu_2O(111)$ showed that the surface conductivity changed as a function of exposure to air or heating in vacuum.[6] One study concluded that the conductivity of Cu_2O single crystals is associated with intrinsic crystal defects, and not due to the presence of oxygen at higher partial pressure.[7] However, Toth *et al.* reported that the conductivity of Cu_2O single crystals depends on the partial pressure of gas-phase oxygen.[8] Assismos and Trivich examined the photoelectric threshold, work function, and surface barrier potential for $Cu_2O(111)$ single crystal surfaces. They concluded that, despite different surface-preparation conditions, the bands for the $Cu_2O(111)$ single-crystal surface remained in a nearly-flat-band condition ($-0.02\le qV_s\le0.13$ eV).[9]

Several theoretical investigations of the band structure of Cu_2O have been reported due to interest in the exciton spectrum. Dahl and Switendick used a non-self-consistent augmented-plane-wave (APW) method and concluded that the exciton spectrum was due to copper-derived electronic states.[10] Kleinman and Mednick[11] used a self-consistent expansion in Gaussian orbitals, and found that spin-orbit splitting puts the $\Gamma^+7(j=\frac{1}{2})$ level above the $\Gamma^+8(j=\frac{3}{2})$ level, in agreement with an earlier interpretation of exciton data.[12] Using a tight-binding Green's-function method, Robertson's calculations gave a band structure more closely resembling the experimental optical gap and the O $2p$ bandwidth than earlier calculations.[13]

Previous studies of polycrystalline copper oxides have shown that Cu^0, Cu^{1+}, and Cu^{2+} can be distinguished using x-ray photoelectron spectroscopy (XPS).[14–17] Cu^{2+} gives rise to intense shake-up features in the Cu $2p$ spec-

 ©1991 The American Physical Society

trum. Cu^0 and Cu^{1+} may be distinguished by differences in the peak position and shape of the Cu L_3VV Auger signal. In addition to differences in the core-level spectra, ultraviolet photoelectron spectroscopy (UPS) can also be used to distinguish between Cu valence states in copper oxide materials.[18]

Rosencwiag and Wertheim examined oxygen and water adsorption on Cu_2O films and identified three different types of oxygen with XPS: lattice oxygen (O^{2-}, $E_b=530.4$ eV), the surface hydroxide ion (OH^-, $E_b=531.4$ eV), and strongly chemisorbed oxygen (O^-, $E_b=532.2$ eV).[15] In their work, no Cu^{2+} was detected at the surface as a result of exposure to gas-phase oxygen or water vapor.

II. IDEAL SURFACES

As with other cubic crystals, an ideal $Cu_2O(111)$ surface possesses hexagonal symmetry. No single atomic layer parallel to the $Cu_2O(111)$ surface contains both copper cations and oxygen anions. The copper planes parallel to the (111) surface contain four Cu^+ cations per surface unit cell with a 4+ charge. Each copper-containing plane is sandwiched between two oxygen-containing planes. Each of these oxygen-containing planes has one anion per surface unit cell and a 2− charge. Thus, a three-plane repeat unit is necessary to satisfy stoichiometry and charge neutrality. Surface-energy considerations dictate that the termination for an ideal, stoichiometric $Cu_2O(111)$ surface be nonpolar.[19] Therefore, the ideal surface will be terminated by an outer atomic layer of oxygen anions, with a second atomic layer of Cu^+ cations, and a third atomic layer of oxygen anions. A ball-model illustration of the ideal, stoichiometric (111) surface is shown in Fig. 1(a). Both singly and doubly coordinated cations can be seen in the second atomic layer.

The ideal $Cu_2O(100)$ surface is polar with square symmetry. As on the (111) surface, no single atomic layer parallel to the (100) surface contains both oxygen anions and copper cations. The bulk structural arrangement perpendicular to the [100] direction alternates between copper- and oxygen-containing planes. The oxygen planes parallel to the $Cu_2O(100)$ surface contain one oxygen anion per (100) surface unit cell with a charge of 2−, while the copper planes are composed of two copper cations per unit cell with a total charge of 2+. Thus, a two-plane repeat unit consisting of one plane of copper and one of oxygen is necessary to maintain stoichiometry and charge neutrality.

An ideal $Cu_2O(100)$ surface should be either copper or oxygen terminated; if it is copper terminated on one side of the crystal, charge neutrality mandates that the opposite side of the crystal be oxygen terminated by analogy to the polar ZnO(0001)-Zn and ZnO(0001)-O surface.[20] Ball-model illustrations of the ideal copper- and oxygen-terminated $Cu_2O(100)$ surfaces are shown in Figs. 1(b) and 1(c), respectively.

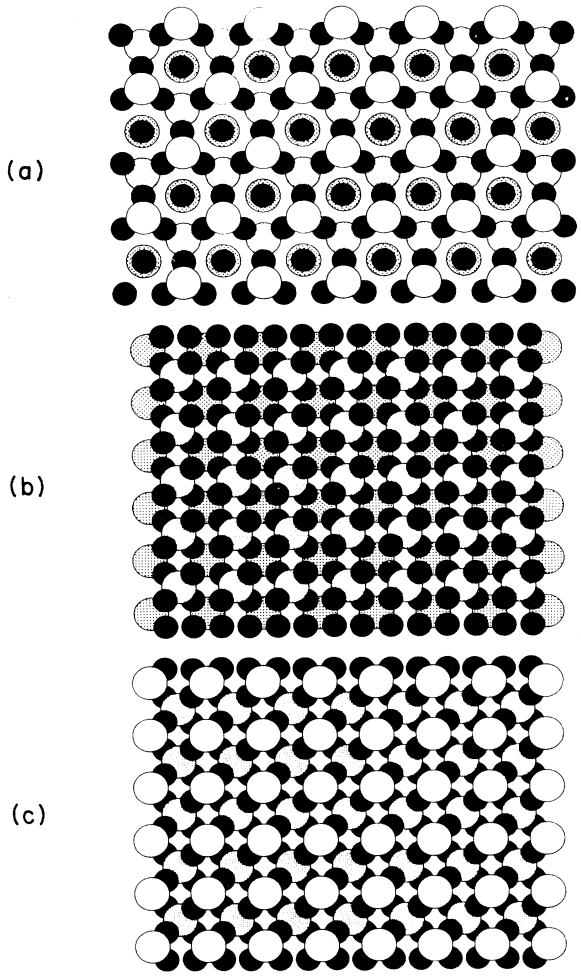

FIG. 1. Ball-model illustrations of (a) the ideal, stoichiometric $Cu_2O(111)$ surface, (b) the ideal, polar, Cu-terminated $Cu_2O(100)$ surface, and (c) the O-terminated $Cu_2O(100)$ surface. The small solid circles represent Cu^+ cations, while the large open circles represent O^{2-} anions. Drawings are based on the ionic radii of the ions, and assume no relaxation. Increased shading of the oxygen anions represents increasing distance away from the surface. For clarity, only the top four atomic layers of each surface are shown.

III. EXPERIMENT

The experimental apparatus used in this study is a dual-chamber, stainless-steel, ultrahigh-vacuum system. The analysis chamber (base pressure 4×10^{-11} Torr) is equipped with a Leybold-Heraeus EA-11 hemispherical energy analyzer, a dual-anode Mg-Al x-ray source for XPS, and a differentially pumped dc discharge lamp for UPS. XPS spectra were collected using Mg $K\alpha$ radiation ($h\nu=1253.6$ eV) exclusively, and run at a resolution of 1.03 eV full width at half maximum (FWHM) on Ag $3d_{5/2}$. UPS spectra were run with an analyzer resolution (ΔE) of 0.15 eV, and referenced to the valence-band maximum.

LEED experiments were performed in the preparation chamber using Vacuum Generators three-grid reverse-view optics. A broad-beam ion gun in the preparation chamber was used for sample cleaning. A high-pressure reaction cell mounted on the preparation chamber was used for large gas exposures. The reaction cell is separated from the rest of the vacuum system by means of sliding seals; thus the sample can be transferred from the reaction cell to the preparation or analytical chambers without exposure to atmosphere. The base pressure of the preparation chamber is 7×10^{-11} Torr.

The sample was clamped to a stainless-steel stage with titanium shims, and could be moved between the two chambers on a sample rod that passed through differentially pumped sliding seals. The sample stage acted both as a mechanical support and an indirect heating and cooling source. A type-*K* thermocouple was fixed between the titanium clamp and the sample stage for temperature measurements. The stage temperature could be varied from 100 to 1000 K. The sample stage and rod construction are such that the stage is permanently grounded. Hence, it was not possible to bias the sample during UPS, thus preventing accurate measures of changes in the sample work function.

The crystals used in this study were grown by a float-zone technique using an arc-image furnace.[21] The 1-mm-thick single crystals were aligned using Laue back-scattering and polished to give an optically smooth surface. An examination of the $Cu_2O(111)$ crystal with LEED showed that the sample contained two rotationally misaligned (111) grains. The center of the crystal showed a superposition of the LEED pattern from each of the grains. One-half of the crystal was azimuthally misaligned from the [111] direction by several degrees and often exhibited split spots, suggesting a stepped surface. All LEED observations described in this paper were made on the opposite, nonstepped half on the $Cu_2O(111)$ crystal, which gave clear LEED patterns with no spot splitting. The (100) surface, in contrast, was a true single crystal aligned to within $\pm0.5°$ of the [100] direction. All the experiments reported for the (100) surface were done only on one side of the crystal. Because of the mechanical mounting procedure, the back of the crystal was sufficiently scratched that it prevented characterization of the opposite side of the (100) polar face.

A variable-leak valve was used to backfill the preparation chamber for exposures up to 10^5 L (1 L$\equiv$1 langmuir$\equiv1\times10^{-6}$ Torr s). Larger doses were done in flowing oxygen at atmospheric pressure in the high-pressure cell. In an effort to minimize water contamination in the oxygen, Matheson research-grade oxygen (99.997% purity) was passed through a stainless-steel coil immersed in liquid nitrogen before entry into a turbo-pumped stainless-steel manifold (base pressure less than 10^{-8} Torr).

IV. RESULTS

A. Ion-bombardment and annealing experiments

Ion-bombardment and consecutive annealing treatments were performed on both surfaces to examine changes in the structure and Cu-to-O ratio upon reordering. After ion bombardment, the samples were heated to successively higher temperatures from 300 to 1000 K in 100-K steps for photoemission and 25-K steps for LEED. All measurements were made after the samples cooled to 300 K.

XPS Cu-to-O ratios were determined from the areas under the Cu $2p_{3/2}$ and O 1*s* peaks and corrected using empirical sensitivity factors appropriate for our analyzer.[22] The major source of error in the XPS Cu-to-O ratios (±0.05) was the determination of the O 1*s* peak area because of the small photoemission cross section relative to Cu. The quoted uncertainty in the CU-to-O ratio (±0.05) reflects *only* the variability in the peak area determinations, *not* the variability of the sample for a given preparation. The Cu-to-O ratios are, therefore, taken to reflect trends in compositional changes at the surface, and not necessarily as absolute measures of the surface composition or stoichiometry.

1. XPS

Variations in the XPS Cu-to-O ratio of the $Cu_2O(111)$ surface are shown in Fig. 2 for a set of ion-bombardment and consecutive annealing experiments. Several sets of data are shown, and although the points show some scatter, no consistent change with annealing temperature in the XPS Cu-to-O ratio is apparent. The data show an average value for the Cu-to-O ratio near 1.75. No change was observed in the Cu 2*p* and the Cu L_3VV Auger signals from that expected for Cu^+. Thus, within the detection limits of XPS, no evidence was seen for either the Cu^{2+} or Cu^0 oxidation states.

Figure 2 also shows the XPS Cu-to-O ratios of the $Cu_2O(100)$ surface for a set of ion-bombardment and consecutive annealing experiments. The Cu-to-O ratio falls in the range 1.5–1.6, and shows little change ($\leq5\%$) with annealing temperature up to 800 K. Upon heating to 900 K, the XPS Cu-to-O ratio decreased from an average value of about 1.57 to about 1.35, indicating an oxidation of the surface by the diffusion of oxygen from the bulk. The Cu-to-O ratio remained at this value, within experimental error, after further annealing to 1000 K. Ion bombardment of the $Cu_2O(100)$ 1000-K-annealed surface with an XPS Cu-to-O ratio of 1.35 returned the XPS Cu-to-O ratio to near 1.60. However, these variations in surface composition proved to be history dependent. After approximately 30 ion-bombardment and annealing treatments, the drop in the Cu-to-O ratio (1.60 to 1.35) at 900 K was no longer observed, and a Cu-to-O ratio near 1.60 was maintained regardless of annealing temperature. The history dependence is apparently related to a depletion of bulk oxygen, which significantly reduces the rate of oxygen diffusion to the surface. No change in the valence state of the Cu atoms at the surface was observed for any of the treatments described above. Thus, as on the (111) surface, no Cu^{2+} or Cu^0 was observed.

2. LEED

After ion-bombarding the $Cu_2O(111)$ surface, a faint (1×1) hexagonal LEED pattern on a diffuse background

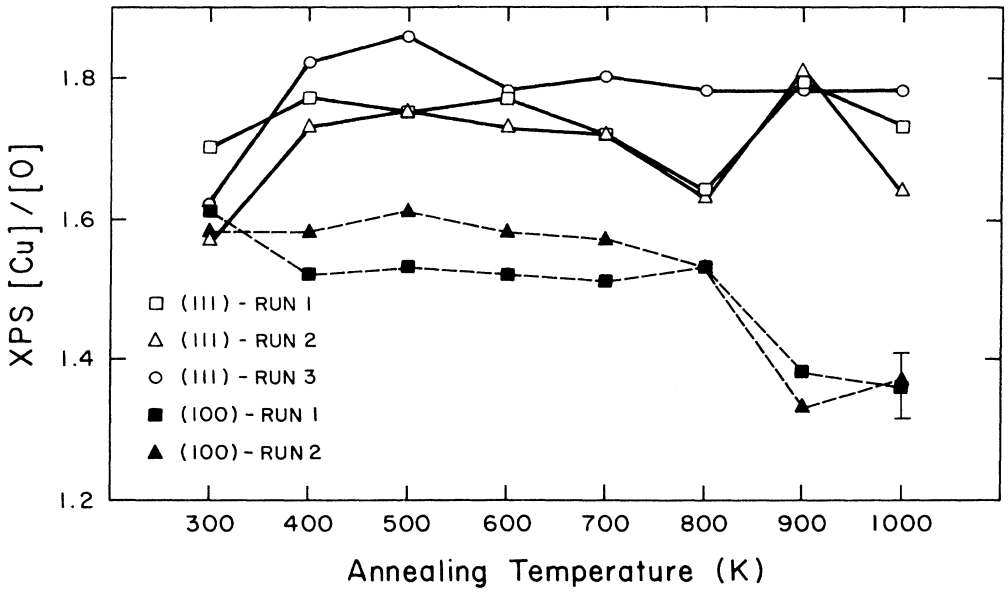

FIG. 2. XPS Cu-to-O ratios for the $Cu_2O(111)$ and (100) surfaces as a function of annealing temperature following ion bombardment. All measurements were made at 300 K following annealing at a given temperature.

was observed, indicating substantial surface disorder. Upon annealing to 550 K, the diffuse background decreased, and faint fractional-order spots were observed in a $(\sqrt{3}\times\sqrt{3})R30°$ periodicity. These faint fractional-order spots would fade if left in the electron beam for 3–5 min. However, no corresponding intensity decrease was observed for the integral-order beams. Further annealing to 950 K sharpened the integral-order beams, and the fractional-order spots disappeared completely. The (1×1) hexagonal pattern for a 1000-K-annealed $Cu_2O(111)$ surface is shown in Fig. 3(a).

Following ion bombardment of the $Cu_2O(100)$ surface, a faint, square (1×1) LEED pattern on a diffuse background was observed, indicating a substantially disordered surface. Upon annealing to 475 K, the integral-order beams became sharper, and faint fractional-order spots became visible. The observed pattern, an apparent $(3\sqrt{2}\times\sqrt{2})R45°$ periodicity *with many missing spots,* became sharpest after annealing at 800 K, and is shown in Fig. 3(b). This periodicity, despite the missing spots, is hereafter referred to as $(3\sqrt{2}\times\sqrt{2})R45°$ for notational convenience. For the initial runs, further annealing to 1000 K resulted in the appearance of an additional *centered* spot with a $(\sqrt{2}\times\sqrt{2})R45°$ periodicity [shown in Fig. 3(c)] concurrent with the drop in the Cu-to-O ratio from 1.60 to 1.35 observed in XPS. However, this high-temperature behavior proved to be history dependent. After approximately 30 ion-bombardment and annealing treatments, the centered spot no longer appeared for annealing temperatures above 800 K. Additionally, the Cu-to-O ratio remained near 1.60 rather than decreasing to 1.35. Thus, the appearance of the centered spot in the LEED pattern was directly related to the change in the Cu-to-O ratio from near 1.60 to 1.35 observed in XPS. For notational purposes, the LEED periodicity shown in Fig. 3(c) is hereafter referred to as a $(3\sqrt{2}\times\sqrt{2})(\sqrt{2}\times\sqrt{2})R45°$ periodicity.

3. *UPS*

UPS ion-bombardment and annealing sequences were performed to check for changes in the valence-band structure as the surfaces reordered. For the $Cu_2O(111)$ surface, no significant changes in the valence-band spectra were observed as a function of annealing temperature.

For the $Cu_2O(100)$ surface, the history dependence of the sample behavior observed in XPS and LEED was also found for UPS. The solid curve in Fig. 4(a) is typical of previously reported HeII spectra of Cu_2O,[18] and corresponds to a 1000-K-annealed surface following many ion-bombardment and annealing cycles (i.e., XPS $[Cu]/[O]\approx1.60$, $(3\sqrt{2}\times\sqrt{2})R45°$ LEED periodicity with no centered spot). Features in the photoemission spectrum from 5 to 8 eV are primarily O $2p$ derived, while the density of states in the 1–4-eV range are primarily Cu $3d$ bands.[13,18] The low-binding-energy feature below 1 eV near the valence-band maximum is associated with Cu d,s,p and O p interactions.

An unusual feature not reported in earlier UPS investigations of polycrystalline Cu_2O (Refs. 14 and 18) was observed at a binding energy of 9.4 eV. The long-term variability of this feature correlates with the behavior observed in XPS and LEED. Figure 4(a) shows a comparison of UPS spectra for two surfaces prepared by ion bombardment and annealing to 1000 K. The dashed curve in Fig. 4(a) corresponds to an early 1000-K-annealed surface following only about 10 ion-bombardment and annealing cycles (i.e., XPS $[Cu]/[O]\approx1.35$, $(3\sqrt{2}$

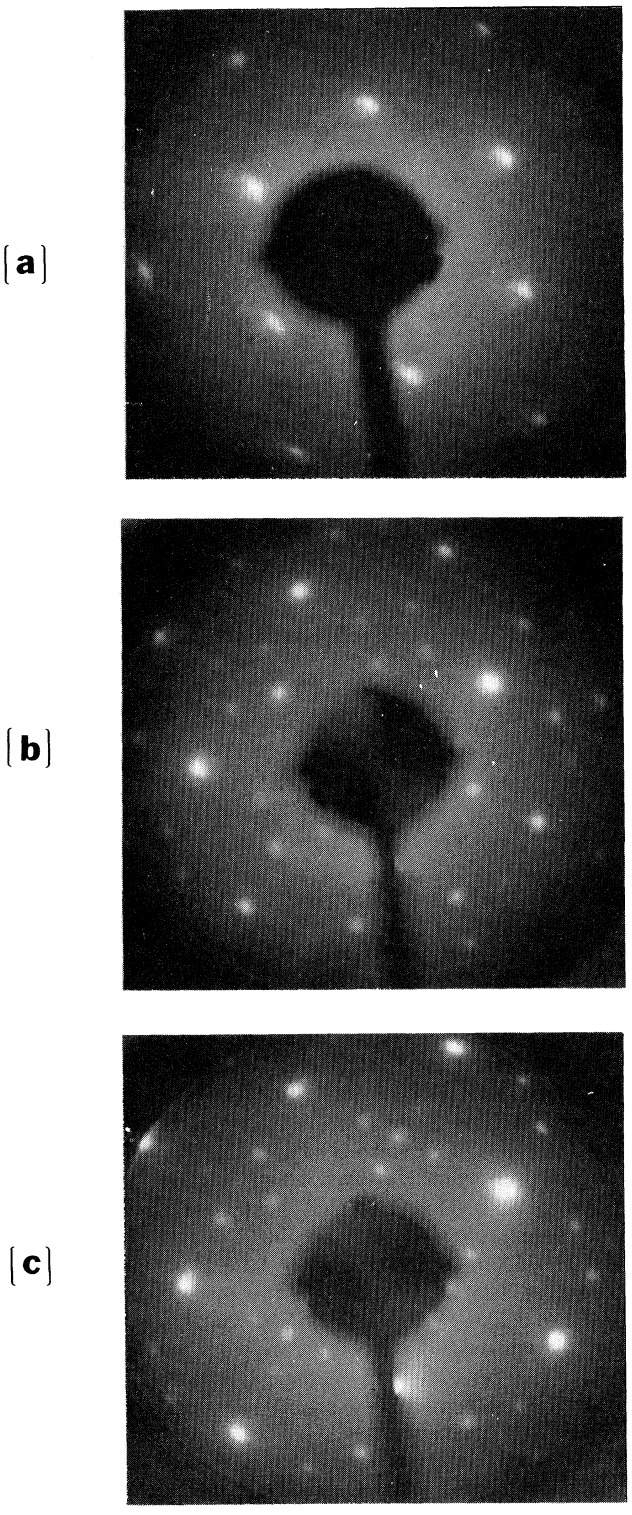

FIG. 3. (a) (1×1) hexagonal LEED pattern ($E_b = 35$ eV) for the $Cu_2O(111)$ surface following ion bombardment and annealing to 1000 K. (b) $(3\sqrt{2}\times\sqrt{2})R45°$ LEED periodicity ($E_b = 35$ eV) for the $Cu_2O(100)$ surface following ion bombardment and annealing to 800 K. (c) $(3\sqrt{2}\times\sqrt{2})(\sqrt{2}\times\sqrt{2})R45°$ pattern ($E_b = 40$ ev) formed by annealing the surface in (b) to 1000 K.

$\times\sqrt{2})(\sqrt{2}\times\sqrt{2})R45°$ LEED periodicity).

For the early runs, where the decrease in the Cu-to-O ratio in XPS and the appearance of the centered spot in LEED were observed following high-temperature annealing, the intensity of the 9.4-eV feature was found to vary significantly as a function of annealing temperature following ion bombardment. This behavior is illustrated in the inset of Fig. 4. A maximum intensity of the 9.4-eV feature occurred after heating the ion-bombarded surface to 400 K. The intensity then decreased continually to zero upon heating to 800 K. Upon annealing to 900 K, the feature again appeared, coincident with a drop in the Cu-to-O ratio from 1.60 to 1.35 and the appearance of a centered spot in the LEED pattern. Figure 4(b) illustrates the maximum variation for a given ion-bombardment and annealing series between the 400-K- (dashed curve) and 800-K- (solid curve) annealed surfaces.

In an effort to identify the 9.4-eV photoemission feature, UPS difference curves were generated between spectra that exhibited a significant difference in intensity of the 9.4-eV feature. A representative difference curve, generated using the two He II spectra in Fig. 4(b) is shown in Fig. 4(c). Regardless of the sample history of the two curves used to generate a difference spectrum, the 9.4-eV feature was always found to be one feature of a difference spectrum like that shown in Fig. 4(c). Agreement was found in the number and positions of the features regardless of whether He I or He II was used as the excitation source. Besides the 9.4-eV feature, a broad feature with a peak at 5.2 eV and a shoulder to higher binding energies (near 7 eV) is also apparent. This broad feature falls in the range of the O $2p$ emission in the $N(E)$ spectrum. An additional feature is also apparent at about 2.3 eV binding energy regardless of data treatment. However, the shape of this low-binding-energy feature is dependent on the shift employed to account for band bending (0.2 eV maximum) as well as any normalization of the spectra prior to taking the difference (for example, no normalization, normalization on the Cu $3d$ bands near 2.5 eV, or normalization on the peak near the valence-band maximum).

B. Oxygen adsorption

Photoemission and LEED were used to investigate the effects of oxygen adsorption at 300 K on both the $Cu_2O(111)$ and $Cu_2O(100)$ surfaces for several different surface preparations. Oxygen doses were started at 0.1 L and increases in order-of-magnitude steps up to 10^9 L. He I and He II were used for UPS, and Cu-to-O ratios were determined with XPS for each exposure. LEED observations were made as a function of annealing temperature following a 10^9-L oxygen dose on the annealed surfaces. All photoemission measurements and LEED observations were made at 300 K. Figure 5 provides an illustrative set of UPS difference curves that are characteristic of the observations made for all surfaces and preparation conditions. For comparison, Fig. 5(a) shows the gas-phase UPS spectrum for molecular oxygen, O_2, reproduced from Ref. 34.

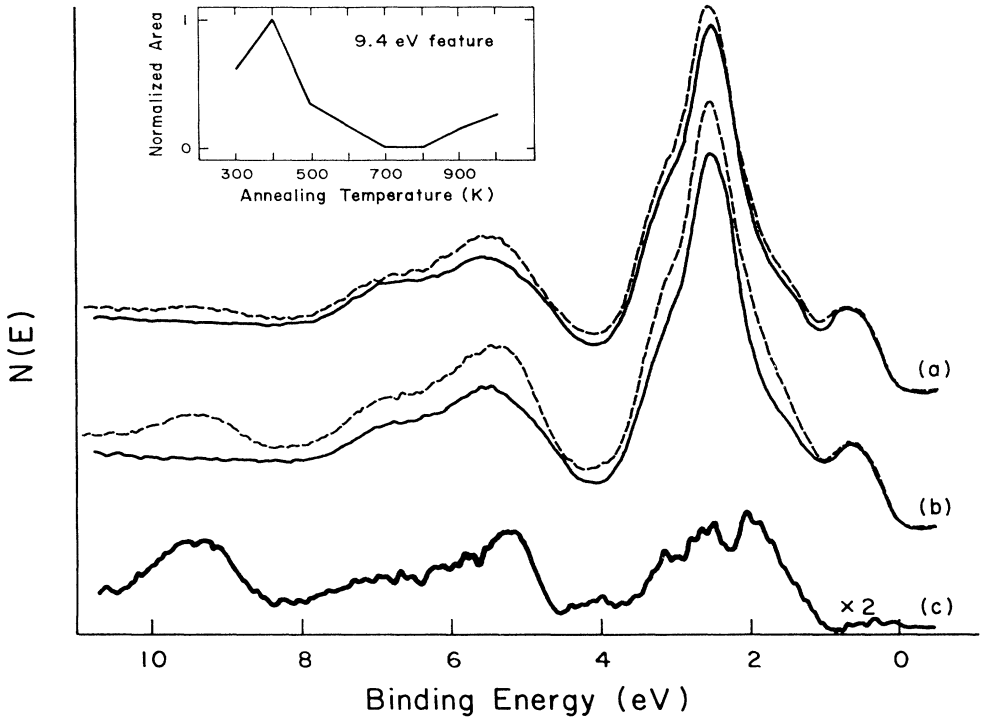

FIG. 4. (a) He II UPS spectra of 1000-K-annealed $Cu_2O(100)$ surfaces. The solid-line spectrum is characteristic of the surface following many ion-bombardment and annealing cycles [$(3\sqrt{2}\times\sqrt{2})R45°$ periodicity], while the dashed spectrum was obtained early in the sample history [$(3\sqrt{2}\times\sqrt{2})(\sqrt{2}\times\sqrt{2})R45°$ periodicity]. (b) He II UPS spectrum of the $Cu_2O(100)$ surface following ion bombardment and annealing to 400 K (dashed) and 800 K (solid). The spectra correspond to the maximum variation in the 9.4-eV photoemission feature for a given ion-bombardment and annealing cycle as shown in the inset. (c) UPS difference curve between the spectra in (b). All spectra are referenced to the valence-band maximum, and $N(E)$ spectra have been normalized on the feature below 1 eV.

1. Oxygen on $Cu_2O(111)$

Two different $Cu_2O(111)$ surface preparations were studied: a (1×1) surface prepared by ion bombardment and annealing to 1000 K for 20 min, and an ion-bombarded surface. No adsorbate-induced features were discernable in UPS on either the ion-bombarded or 1000-K-annealed (1×1) surfaces for oxygen exposures of less than 10^4L. For 10^4-L exposures, the hexagonal, 1000-K-annealed (1×1) surface exhibited a two-peaked UPS difference spectrum with a peak separation of 4.6 eV, as shown in Fig. 5(b). In contrast, oxygen adsorption on the ion-bombarded surface gave rise to the difference spectrum shown in Fig. 5(c) with maxima at 9.4, 5.2, and 2.3 eV, and a shoulder at about 7 eV. For comparison purposes, the spectrum from Fig. 4(c) is reproduced as Fig. 5(d). A comparison of Figs. 5(c) and 5(d) demonstrates the electronic similarity between the oxygen-adsorption-induced features on the ion-bombarded (111) surface and the (100) surface under conditions when the 9.4-eV photoemission feature is observed.

2. Oxygen on $Cu_2O(100)$

Four different $Cu_2O(100)$ surface conditions were studied: an ion-bombarded surface, an 800-K-annealed $(3\sqrt{2}\times\sqrt{2})R45°$ surface, a 1000-K-annealed $(3\sqrt{2}\times\sqrt{2})(\sqrt{2}\times\sqrt{2})R45°$ surface, and a 1000-K-annealed $(3\sqrt{2}\times\sqrt{2})R45°$ surface formed after more than 30 ion-bombardment and annealing treatments. The different (100) surface preparations were chosen because of the different XPS Cu-to-O ratios and LEED patterns observed for these conditions.

No new valence-band features were observed for any of the four $Cu_2O(100)$ surface preparations for oxygen exposures up to 10^4L. For each of the four surface preparations investigated, a UPS difference spectrum essentially identical to that obtained for oxygen adsorption on the ion-bombarded $Cu_2O(111)$ surface [Fig. 5(c)] was obtained. Further oxygen exposures to 10^9 and above gave similar difference spectra, with some increased intensity, but no new features.

For each (100) surface preparation investigated, *except ion bombardment,* a (1×1) square LEED pattern with diffuse background and a XPS Cu-to-O ratio of about 1.15 was observed after a 10^9-L dose of oxygen. A representative (1×1) square LEED pattern is shown in Fig. 6(a). When heated to 400–450 K in vacuum, the (1×1) surfaces formed by 10^9-L oxygen exposures at 300 K exhibited $(\sqrt{2}\times\sqrt{2})R45°$ LEED periodicities [shown in Fig. 6(b)] with XPS Cu-to-O ratios of about 1.35. Annealing in vacuum to temperatures above 500 K led to

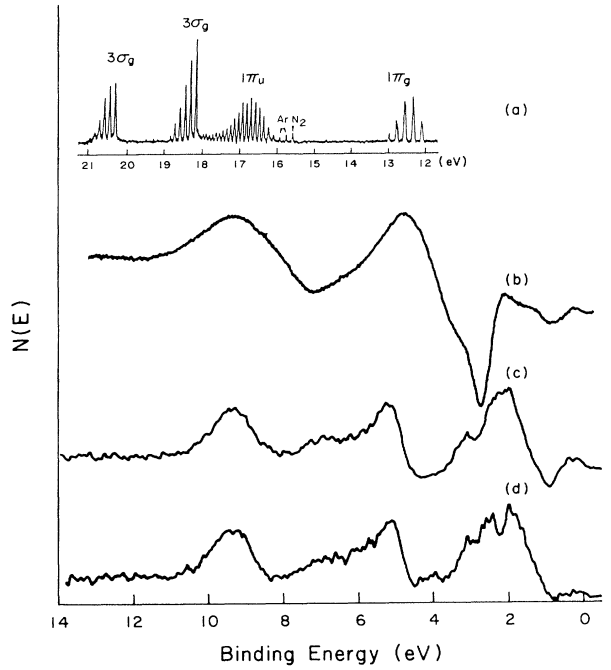

FIG. 5. (a) Gas-phase O_2 UPS spectrum reprinted from Ref. 34 by permission of John Wiley & Sons, Ltd. (b) He I UPS difference spectrum of oxygen adsorbed on the (1×1), 1000-K-annealed, $Cu_2O(111)$ surface. (c) He II difference spectrum following a 10^4-L O_2 exposure on the ion-bombarded $Cu_2O(111)$ surface. Similar spectra to (c) are also observed following oxygen adsorption on all $Cu_2O(100)$ surface preparations investigated (see text for details). (d) Figure 4(c) difference spectrum, reproduced for comparison. All spectra except (a) are referenced to the valence-band maximum.

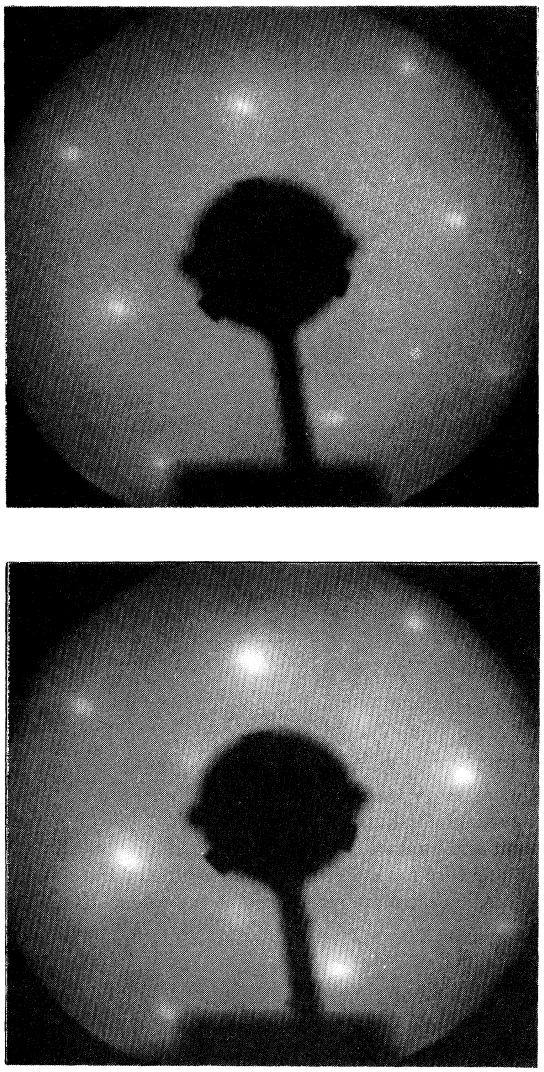

FIG. 6. (a) Square (1×1) pattern observed following 10^9-L oxygen dose on an ordered $Cu_2O(100)$ surface. (b) $(\sqrt{2}\times\sqrt{2})R45°$ periodicity observed following annealing of the surface in (a) to 400–450 K. All beam energies were 40 eV.

complete removal of adsorbed oxygen, as evidence by a return to the original LEED periodicity and XPS Cu-to-O ratio for a given starting condition.

V. DISCUSSION

A. Surface structure

1. $Cu_2O(111)$

The LEED observations for the (111) surface suggest the possibility of two different surface terminations corresponding to a hexagonal (1×1) periodicity and a $(\sqrt{3}\times\sqrt{3})R30°$ LEED periodicity. While only a faint $(\sqrt{3}\times\sqrt{3})R30°$ pattern was observed during the course of ion-bombardment and annealing studies, a much sharper and more distinct $(\sqrt{3}\times\sqrt{3})R30°$ pattern has been observed during studies of the catalytic chemistry of $Cu_2O(111)$ resulting from repeated exposures to propene ($CH_3CH=CH_2$) during thermal-desorption spectroscopy (TDS).[23] The observation of trace amounts of CO as a reaction-limited product in each TDS run suggests a net surface reduction (i.e., oxygen removal) associated with the $(\sqrt{3}\times\sqrt{3})R30°$ periodicity.[23]

A $(\sqrt{3}\times\sqrt{3})R30°$ periodicity is typically associated with $\frac{1}{3}$ monolayer of adsorbed species on hexagonal substrates.[24] For the $Cu_2O(111)$ surface that exhibits a loss of oxygen, domains of $(\sqrt{3}\times\sqrt{3})R30°$ periodicity could be indicative of the ordered loss of $\frac{1}{3}$ or $\frac{2}{3}$ of the terminating layer of oxygen anions from a stoichiometric surface. The change in LEED pattern from a (1×1) to a $(\sqrt{3}\times\sqrt{3})R30°$ surface occurs gradually, with faint fractional-order spots appearing over the course of about 20 propene TDS runs. The slow rate of change to the new periodicity, coupled with the observation of only trace amounts of CO per run, suggests that $\frac{1}{3}$ (rather than $\frac{2}{3}$) of the terminating oxygen layer is removed to form $(\sqrt{3}\times\sqrt{3})R30°$ periodicity.[23] Oxygen-vacancy formation is supported by the observation of an additional, higher-

temperature propene desorption channel in TDS from $Cu_2O(111)$ surfaces exhibiting $(\sqrt{3}\times\sqrt{3})R30°$ LEED periodicities.[23]

Note that for the $(\sqrt{3}\times\sqrt{3})R30°$ surface observed in the ion-bombardment (Sec. IV A) and surface chemistry[23] studies, no significant increase in the XPS Cu-to-O ratio has been observed, in apparent conflict with the proposed model requiring an ordered $\frac{1}{3}$ of an atomic layer of oxygen vacancies at the surface. However, numerical simulations of the variation in XPS Cu-to-O ratio for normal emission based on the mean-free-path dependence of the photoelectrons (assuming no diffraction effects) gives a decrease in the XPS Cu-to-O ratio of only 0.05 for a surface with $\frac{1}{3}$ of an atomic layer of oxygen vacancies.[25,26] Because this variation is within experimental error, the use of our normal-emission XPS data for evaluating this oxygen-vacancy model of the (111) surface is problematic.

The (1×1) LEED periodicity for the 1000-K-annealed $Cu_2O(111)$ surface suggests a more nearly ideal, stoichiometric surface than the $(\sqrt{3}\times\sqrt{3})R30°$ surface. A (1×1) LEED periodicity is characteristic of a simple, though not necessarily stoichiometric, termination of the bulk. An estimate of the defect (oxygen-vacancy) density in the top atomic layer has been made via TDS experiments using propene as a probe molecule.[23] Assuming that a sharp, well-defined , $(\sqrt{3}\times\sqrt{3})R30°$ periodicity is characteristic of $\frac{1}{3}$ of an atomic layer of oxygen vacancies, a comparison of the relative intensity of the high-temperature propene desorption state for a (1×1) surface prepared by ion bombardment and annealing gives an estimate of about 3% oxygen vacancies in the top atomic layer. Thus, the (1×1) surface condition resulting from ion bombardment and annealing to 1000 K can be described as nearly stoichiometric, and the corresponding surface structure should be similar to the ideal stoichiometric surface shown in Fig. 1(a), assuming no relaxation. Herion *et al.*[4] have reported that stoichiometric $Cu_2O(111)$ surfaces can be prepared by ion-bombarding and annealing in vacuum to at least 425 K. However, our LEED observations (fractional-order spots until 950 K) demonstrate that much higher temperatures are required to completely order the surface.

2. $Cu_2O(100)$

Four different LEED patterns have been observed on the (100) surface: (1×1), $(\sqrt{2}\times\sqrt{2})R45°$, $(3\sqrt{2}\times\sqrt{2})(\sqrt{2}\times\sqrt{2})R45°$, and $(3\sqrt{2}\times\sqrt{2})R45°$ periodicities. The observation of distinct and separate $(3\sqrt{2}\times\sqrt{2})R45°$ and $(\sqrt{2}\times\sqrt{2})R45°$ periodicities [Figs. 3(b) and 6(b), respectively] for different preparation conditions suggest that the $(3\sqrt{2}\times\sqrt{2})(\sqrt{2}\times\sqrt{2})R45°$ pattern [Fig. 3(b)] is a combination of domains with the two different periodicities. The XPS Cu-to-O ratios observed with the different periodicites vary in the order

$$(3\sqrt{2}\times\sqrt{2})R45° > (3\sqrt{2}\times\sqrt{2})(\sqrt{2}\times\sqrt{2})R45° \approx (\sqrt{2}\times\sqrt{2})R45° > (1\times1)\ ,$$

with values of about 1.60, 1.35, and 1.15, respectively.

Calculations of the expected variation in XPS Cu-to-O ratio for the two ideal terminations of the polar (100) surface give values of 1.57 for the Cu-terminated surface [Fig. 1(b)] and 1.23 for the O-terminated surface [Fig. 1(c)].[25,26] While there is much uncertainty in the appropriate values of mean free paths to use for such calculations, the similarity between the experimentally measured extremes in Cu-to-O ratio (1.60 and 1.15) and the calculated values for the two ideal surfaces (1.57 and 1.23) suggest that models *compositionally* similar to the ideal surfaces (i.e., copper and oxygen terminated) be considered to describe the $(3\sqrt{2}\times\sqrt{2})R45°$ and (1×1) LEED periodicities.

The (1×1) LEED periodicity observed after a 10^9 L exposure of oxygen on the (100) surface is characteristic of a simple termination of the bulk, and demonstrates that oxygen adsorption lifts the $(3\sqrt{2}\times\sqrt{2})R45°$ reconstruction observed for the most oxygen-deficient (100) surface. The UPS data demonstrate that the adsorbed oxygen species on the (100) surfaces are atomic (see Sec. V B), and therefore suggest a surface structurally and compositionally similar to an ideal, oxygen-terminated (100) surface.[25] This assignment is further supported by the observation of a $(\sqrt{2}\times\sqrt{2})R45°$ pattern formed by heating the (1×1) surface and partially desorbing the adsorbed oxygen layer. The $(\sqrt{2}\times\sqrt{2})R45°$ periodicity is suggestive of the presence (or absence) of $\frac{1}{2}$ of a terminating oxygen layer, thus demonstrating that the (1×1) pattern is associated with a significantly higher surface oxygen coverage approaching that of a nearly complete terminating layer of oxygen atoms.

Annealing a (100) surface exhibiting a $(\sqrt{2}\times\sqrt{2})R45°$ periodicity (formed by a 10^9-L O_2 exposure and heating in vacuum to 400–450 K) leads to the appearance of a $(3\sqrt{2}\times\sqrt{2})R45°$ contribution in LEED. The final periodicity observed following high-temperature annealing in vacuum is the same as the initial starting condition prior to oxygen dosing, and displays either a $(3\sqrt{2}\times\sqrt{2})(\sqrt{2}\times\sqrt{2})R45°$ or $(3\sqrt{2}\times\sqrt{2})R45°$ periodicity, depending on the sample history. Regardless of the method of preparation, (100) surfaces exhibiting a $(\sqrt{2}\times\sqrt{2})R45°$ contribution in the LEED periodicity have XPS Cu-to-O ratios which fall essentially midway between those of the (1×1) and $(3\sqrt{2}\times\sqrt{2})R45°$ surfaces. Based on the assumption of an O-terminated (1×1) surface, these observations support the model for a $(\sqrt{2}\times\sqrt{2})R45°$ periodicity associated with $\frac{1}{2}$ of a terminating oxygen layer, and a $(3\sqrt{2}\times\sqrt{2})R45°$ Cu-terminated, reconstructed surface.

The compositional arguments described above are somewhat circular, and depend on the assignment of the surface with the lowest (highest) Cu-to-O ratio to an oxygen (copper) termination. However, we feel the agreement between the compositional data from XPS and structural data from LEED is compelling. It would, however, be advantageous to confirm these structural and compositional models with a direct imaging technique such as scanning tunneling microscopy.

Describing the $Cu_2O(100)$ Cu-terminated, reconstructed surface as a $(3\sqrt{2}\times\sqrt{2})R45°$ periodicity is notationally convenient, but not correct since there are many miss-

ing spots. The true periodicity is best described in terms of two rotational domains of an oblique lattice at 90° angles. One lattice vector is identical to that of the principle lattice vector of an unreconstructed surface (i.e., along the [010] or [00$\bar{1}$] directions), while the second lattice vector is oriented 45° off the first (i.e., along the [011] or [01$\bar{1}$] directions) with a magnitude of $\frac{3}{2}\sqrt{2}$. The oblique lattice vectors of the two domains map out all the spots in the observed LEED pattern without requiring additional unobserved spots. These oblique lattice vectors and the corresponding domains are shown superimposed on an ideal, Cu-terminated, $Cu_2O(100)$ surface in Fig. 7.

The observed reconstruction of the Cu-terminated $Cu_2O(100)$ surface is not surprising since ideal polar surface exhibit high surface energies, and thus are often unstable.[19] For example, the relaxation of the Zn-terminated ZnO(0001) polar surface is well known.[27] One possible explanation for the oblique [i.e., $(3\sqrt{2}\times\sqrt{2})R45°$] lattice on the Cu-terminated $Cu_2O(100)$ surface is a relaxation of the singly coordinated surface copper cations. Such a model is suggested by the $\frac{3}{2}\sqrt{2}$ lattice vectors along the [011] and [01$\bar{1}$] directions. The $\frac{3}{2}\sqrt{2}$ dimension is an integer multiple of the $\frac{1}{2}\sqrt{2}$ separation between the Cu cations along these directions for the ideal, unreconstructed surface as shown in Fig. 7, but is not an integer multiple of the $\sqrt{2}$ spacing between anions along these directions. A relaxation between adjacent copper cations in neighboring rows along the [011] or [01$\bar{1}$] directions in steps of $(\frac{3}{2})\sqrt{2}$ satisfies the oblique periodicity and requires only a single type of Cu^+-Cu^- interaction. No relaxation is suggested for copper cations along the same [011] or [01$\bar{1}$] rows because the periodicity would require two different Cu^+-Cu^+ interactions: (1) between cations bound to the same second-layer oxygen anion, and (2) cations bound to neighboring second-layer oxygen anions.

Such a relaxation can be rationalized in terms of Cu^+-Cu^+ bonding on the $Cu_2O(100)$ surface similar to that observed between Cu^+ centers in organometallic compounds, where a tendency for clustering is observed for Cu^+ cations. Using molecular-orbit calculations, Mehrotra and Hoffmann found that despite a closed-shell d^{10} configuration, a small bonding interaction between bare Cu^+ cations occurs because of hybridized 4*s*, 4*p*, and 3*d* orbitals.[28] They also report that typical Cu^+-Cu^+ distances in organometallic compounds range from 3.58 to 2.42 Å. The Cu^+-Cu^+ distance for an ideal, unrelaxed, Cu-terminated (100) surface is 3.01 Å,[2] which falls well within the ranges of separations reported for organometallic complexes.

Mehrotra and Hoffmann also report that bridging ligands play the dominant role in determining geometry and bond angles in copper-containing organometallic compounds.[28] The Cu-terminated $Cu_2O(100)$ surface possesses a high concentration of unsaturated Cu^+ cations essentially "missing" an oxygen ligand, thus supporting the possibility of a Cu^+-Cu^+ interaction affecting the structure of a Cu-terminated $Cu_2O(100)$ surface. The presence of Cu^+-Cu^+ bonding to account for the oblique periodicity is also supported with the lifting of the reconstruction with $\frac{1}{2}$ of an atomic layer of oxygen ligands in a $(\sqrt{2}\times\sqrt{2})R45°$ surface. An ordered $\frac{1}{2}$ monolayer of oxygen is enough to tie up at least one interacting Cu^+ cation per Cu^+-Cu^+ bonding pair and, hence, plays the dominant role in determining the surface structure.

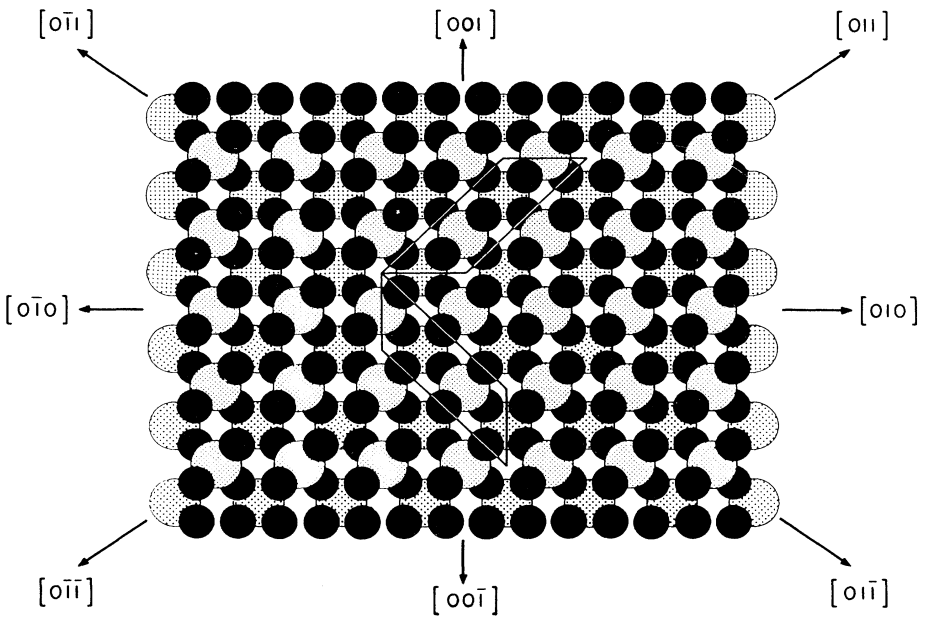

FIG. 7. Ball-model drawing of the ideal, Cu-terminated $Cu_2O(100)$ surface showing the two rotational domains of oblique periodicity corresponding to the $(3\sqrt{2}\times\sqrt{2})R45°$ LEED pattern shown in Fig. 3(b).

B. Identification of surface oxygen species

1. Oxygen adsorption on the 1000-K annealed $Cu_2O(111)$ surface

Oxygen adsorption at 300 K gave a two-peaked UPS difference spectrum [Fig. 5(b)] with a peak separation of 4.6 eV. In previous studies of room-temperature oxygen adsorption on metallic copper surfaces, Spitzer and Lüth[29] reported two UPS features for atomic oxygen with separations of 3.7–4.0 eV, depending on the surface under study. The significantly larger peak separation in our data suggest that a different explanation is required.

Room-temperature adsorption of oxygen on several other materials, primarily metal oxides, has been found to yield two-peaked UPS difference spectra with separations similar to those observed on the nearly stoichiometric $Cu_2O(111)$ surface. Such two-peaked spectra have been observed on GaAs(100),[30] $SrTiO_3(100)$,[31] NiO(100),[32] and MnO(100),[33] with peak separations of 4.6, 4.5, 5.0, and 4.1 eV, respectively. In each case the adsorbed specie has been identified as molecular oxygen.

Neutral O_2 in the gas phase displays a characteristic UPS spectrum with four peaks as shown in Fig. 5(a).[34] The four photoemission features are due to $1\pi_g$ and $1\pi_u$ orbitals, and two different final states of $3\sigma_g$ emission.[34] It has been proposed that a two-peaked spectrum for adsorbed molecular oxygen may be due to overlap of $1\pi_u$ and $3\sigma_g$ orbitals giving the high-binding-energy peak, with the $1\pi_g$ orbital giving the low-binding-energy peak.[30,32] McKay and Henrich[32] have attributed this overlap to a relaxation of the O—O bond associated with a negatively charged molecular adsorbate, possibly O_2^{2-}. The broadness of the peaks observed in the UPS difference spectrum for oxygen adsorption on nearly stoichiometric $Cu_2O(111)$ [Fig. 5(b)] is consistent with such an interpretation. The separation between the $3\sigma_g$ and $1\pi_u$ orbitals is slightly less than 2 eV in the gas phase. However, the width of the associated photoemission feature in the difference spectrum is also about 2 eV, implying that the two features observed in the gas phase are not resolved in the adsorbate. Thus, the two-peaked UPS difference spectrum in Fig. 5(b) is assigned to adsorbed molecular oxygen.

2. Oxygen adsorbed on $Cu_2O(100)$ and ion-bombarded $Cu_2O(111)$

Oxygen adsorption at room temperature on all (100) surfaces and the ion-bombarded (111) surface results in UPS difference spectra with four features [Fig. 5(c)]. Essentially identical features were observed for the surface species formed by diffusion of bulk lattice oxygen to the $Cu_2O(100)$ surface at elevated temperatures for the early sample treatments [Fig. 5(d)]. Despite the similar number of features, there is no clear correspondence with the four-peaked gas-phase spectrum for molecular oxygen. Comparisons to data for oxygen adsorption on metallic copper show no clear correspondence in terms of peak separations or binding energies to the two- and three-peaked spectra assigned to triplet atomic oxygen and singlet molecular oxygen, respectively.[29,35,36]

Consideration of the oxygen-induced features at intermediate binding energies leads to the conclusion that atomic oxygen species give rise to the difference spectra in Figs. 5(c) and 5(d). The peak at 5.2 eV and the shoulder near 7 eV show a strong correspondence in position and relative intensity with the O $2p$ features of the oxide substrate, indicating oxygen dissociation and at least partial incorporation as lattice oxygen, O^{2-}.

The low-binding-energy feature at 2.3 eV clearly is oxygen induced, but its origins are unclear. Tight-binding calculations of the bulk-electronic structure of Cu_2O have shown that a contribution of O $2p$ states is expected for lattice oxygen in this range of binding energies,[13] consistent with the idea of at least partial incorporation of dissociated oxygen into the lattice. However, some charge redistribution may also be expected between Cu $3d$, $4s$, and $4p$ states as a result of changes in hybridization upon adsorption. This explanation is appealing considering the proposed Cu^+-Cu^+ bonding interaction for the reconstructed, Cu-terminated (100) surface. Unfortunately, while there is clearly an increase in the density of states upon adsorption in this binding-energy range, the variability in shape and intensity of the 2.3-eV feature with different forms of data manipulation (band-bending corrections, normalization versus no normalization, etc.) currently prevents a distinction between such possibilities.

The high-binding-energy peak at 9.4 eV is clearly not associated with lattice oxygen, and suggests the presence of a nonincorporated form of adsorbed oxygen. Since this photoemission feature is observed following ion bombardment or diffusion of bulk oxygen to the (100) surface at high temperatures early in the sample history, it is unlikely that it is associated with a molecular adsorbate. Similarly, the ordering of annealed $Cu_2O(100)$ surfaces to a (1×1) LEED periodicity following large oxygen exposures (10^9 L) is consistent with an atomic adsorbate, which can assume the periodicity expected for a ideal O-terminated (100) surface. Thus, surface oxygen resulting from adsorption on the (100) and ion-bombarded (111) surface or diffusion from the bulk to the (100) surface at high temperature is believed to be atomic, with the photoemission showing characteristics of both adsorbed and incorporated (i.e., lattice) oxygen.

3. Interference from contaminant water

When oxygen-adsorption studies require very large exposures such as those reported here, the possibility of interference from contaminant water must be seriously considered. For this reason, we have studied water adsorption on both the (111) and (100) surfaces of Cu_2O.[23] Water adsorption is dissociative at room temperature and is characterized by a two-peaked UPS difference spectrum with peak separation of 3.7 eV. The UPS results are clearly different than those observed following oxygen ad-

sorption. It is also notable that H_2O adsorption on the reconstructed, Cu-terminated (100) surface does not result in either a lifting of the reconstruction to a (1×1) periodicity or a measurable increase in the Cu-to-O ratio as observed following oxygen adsorption. Thus, it is concluded that the reported results for oxygen adsorption are not merely due to contaminant-water adsorption.

VI. SUMMARY AND CONCLUSIONS

Ion bombardment and 1000-K annealing of the nonpolar $Cu_2O(111)$ surface in vacuum produces a nearly stoichiometric surface. A $(\sqrt{3}\times\sqrt{3})R30°$ periodicity was also observed on the $Cu_2O(111)$ surface, and is tentatively assigned to an ordered $\frac{1}{3}$ of an atomic layer of oxygen vacancies. Oxygen adsorption at room temperature on the stoichiometric surface is molecular, and gives rise to a characteristic two-peak UPS spectrum similar to that observed for other metal oxides. Oxygen adsorption on the defective (111) surface formed by ion bombardment was found to be dissociative. The atomic species on the defective surface show characteristics of both incorporated (i.e., lattice) and adsorbed oxygen.

Ion-bombardment and vacuum-annealing results for the polar $Cu_2O(100)$ surface were history dependent. Annealing the ion-bombarded (100) surface to 800 K in vacuum gave an ordered, reconstructed, Cu-terminated surface with an apparent $(3\sqrt{2}\times\sqrt{2})R45°$ periodicity. The periodicity of the reconstruction suggests a relaxation of singly coordinated, top-atomic-layer Cu^+ cations, possibly associated with weak Cu^+-Cu^+ bonding interactions. For the initial treatments, heating to 900 K resulted in the diffusion of oxygen from the bulk to the surface to form $(\sqrt{2}\times\sqrt{2})R45°$ domains associated with an ordered $\frac{1}{2}$ of an outer atomic layer of oxygen atoms. This surface oxygen exhibited electronic characteristics of both incorporated (i.e., lattice) and adsorbed species. After approximately 30 ion-bombardment and annealing treatments, bulk oxygen was sufficiently depleted such that a $(3\sqrt{2}\times\sqrt{2})R45°$ Cu-terminated surface was retained for annealing temperatures of 900 K and above.

Oxygen adsorption on four differently prepared $Cu_2O(100)$ surfaces was found to be atomic, with photoemission characteristics identical to those observed for oxygen which diffused from the bulk to the surface during high-temperature annealing early in the sample history. Large oxygen exposures (10^9 L) lifted the observed $(3\sqrt{2}\times\sqrt{2})R45°$ reconstruction associated with the Cu-terminated surface to give a (1×1) LEED periodicity and an O-terminated $Cu_2O(100)$ surface. Heating at 400–450 K desorbed half of the terminating layer, leaving an ordered $(\sqrt{2}\times\sqrt{2})R45°$ periodicity. Heating above 500 K removed the remainder of the adsorbed oxygen and returned the surface to its original condition prior to the dose. Oxygen atoms in the outer atomic layer of the (100) surface, whether formed by adsorption or diffusion from the bulk, exhibited photoemission characteristics of both adatoms and lattice oxygen.

ACKNOWLEDGMENTS

We thank Professor L. Tapiero for providing the single crystals used in this study. The support of the U.S. National Science Foundation, under Grant No. CBT-870876, and of the Donors of The Petroleum Research Fund, administered by the American Chemical Society, is gratefully acknowledged.

*To whom correspondence should be addressed.
[1]K. Wandelt, Surf. Sci. Rep. **2**, 1 (1982).
[2]A. F. Wells, *Structural Inorganic Chemistry*, 4th Ed. (Clarendon, Oxford, 1975), p. 935.
[3]P. W. Baumeister, Phys. Rev. **121**, 359 (1961).
[4]J. Herion, G. Scharl, and M. Tapiero, Appl. Surf. Sci. **14**, 233 (1982/83).
[5]G. Panzner, B. Egert, and H. P. Schmidt, Surf. Sci. **151**, 400 (1985).
[6]J. P. Zielinger, M. Tapiero, and C. Noguet, Ann. Phys. (Paris) **7**, 95 (1972).
[7]M. O'Keeffe and W. J. Moore, J. Chem. Phys. **35**, 1324 (1962).
[8]R. S. Toth, R. Kilkson, and D. Trivich, Phys. Rev. B **122**, 482 (1961).
[9]J. A. Assismos and D. Trivich, Phys. Rev. B **122**, 482 (1961).
[10]J. P. Dahl and A. C. Switendick, J. Phys. Chem. Solids **27**, 931 (1966).
[11]I. Kleinman and K. Mednick, Phys. Rev. B **21**, 1549 (1980).
[12]R. J. Elliott, Phys. Rev. **124**, 340 (1961).
[13]J. Robertson, Phys. Rev. B **28**, 3378 (1983).
[14]J. Ghijsen, L. H. Tjeng, J. van Elp, H. Eskes, J. Westerink, G. A. Sawatzy, and M. Y. Czyzyk, Phys. Rev. B **38**, 11 322 (1988).
[15]A. Rosencwiag and G. K. Wertheim, J. Electron Spectrosc. Relat. Phenom. **1**, 493 (1972/73).
[16]K. S. Kim, J. Electron Spectrosc. Relat. Phenom. **3**, 217 (1974).
[17]J. P. Tobin, W. Hirschwald, and J. Cunningham, Appl. Surf. Sci. **16**, 441 (1983).
[18]C. Benndorf, H. Caus, B. Egert, H. Seidel, and F. Theime, J. Electron Spectrosc. Relat. Phenom. **19**, 77 (1980).
[19]P. W. Tasker, J. Phys. C **12**, 4977 (1979).
[20]A. N. Mariano and R. E. Hanneman, J. Appl. Phys. **34**, 384 (1963).
[21]J. L. Loison, M. Robino, and B. Schwab, J. Cryst. Growth **50**, 816 (1980).
[22]Sensitivity factors of 5.3 and 0.61 were used for copper and oxygen, respectively, and were obtained from Leybold Hereaus Vacuum Products.
[23]K. H. Schulz and D. F. Cox (unpublished).
[24]M. A. Van Hove, W. H. Weinberg, and C. M. Chan, *Low Energy Electron Diffraction* (Springer-Verlag, New York, 1986), pp. 73–79.
[25]Estimates of the expected XPS Cu-to-O ratios were calculated assuming (1) an exponential decay of signal intensity with distance for normal emission (2) no diffraction effects, and (3) inelastic mean free paths of 7.5 and 11.0 Å for copper ($E_k \approx 320$ eV) and oxygen photoelectrons ($E_k \approx 720$ eV), respectively

(from the "universal" curve, Ref. 26).
[26]W. M. Riggs and M. J. Parker, in *Methods of Surface Analysis,* edited by A. W. Czanderna (Elsevier, Amsterdam, 1975), p. 103.
[27]A. R. Lubinsky, C. B. Duke, S. C. Chang, B. W. Lee, and P. Mark, J. Vac. Sci. Technol. **13**, 189 (1976).
[28]P. K. Mehrotra and R. Hoffmann, Inorg. Chem. **17**, 2187 (1978).
[29]A. Spitzer and H. Lüth, Surf. Sci. **118**, 121 (1982); **118**, 136 (1982).
[30]W. Ranke and K. Jacobi, Surf. Sci. **81**, 504 (1979).
[31]V. E. Henrich, G. Dresselhaus, and H. J. Zeiger, J. Vac. Sci. Technol. **15**, 534 (1978).
[32]J. M. McKay and V. E. Henrich, Phys. Rev. B **32**, 67 (1985).
[33]R. J. Lad and V. E. Henrich, J. Vac. Sci. Technol. **6**, 781 (1988); R. J. Lad (private communication).
[34]D. W. Turner, C. Baker, A. D. Baker, and C. R. Brundle, *Molecular Photoelectron Spectroscopy* (Wiley, New York, 1970).
[35]K. Prabhakaran, P. Sen, and C. N. R. Rao, Surf. Sci. **177**, L971 (1986).
[36]P. Vishnu Kamath and C. N. R. Rao, J. Phys. Chem. **88**, 464 (1984).

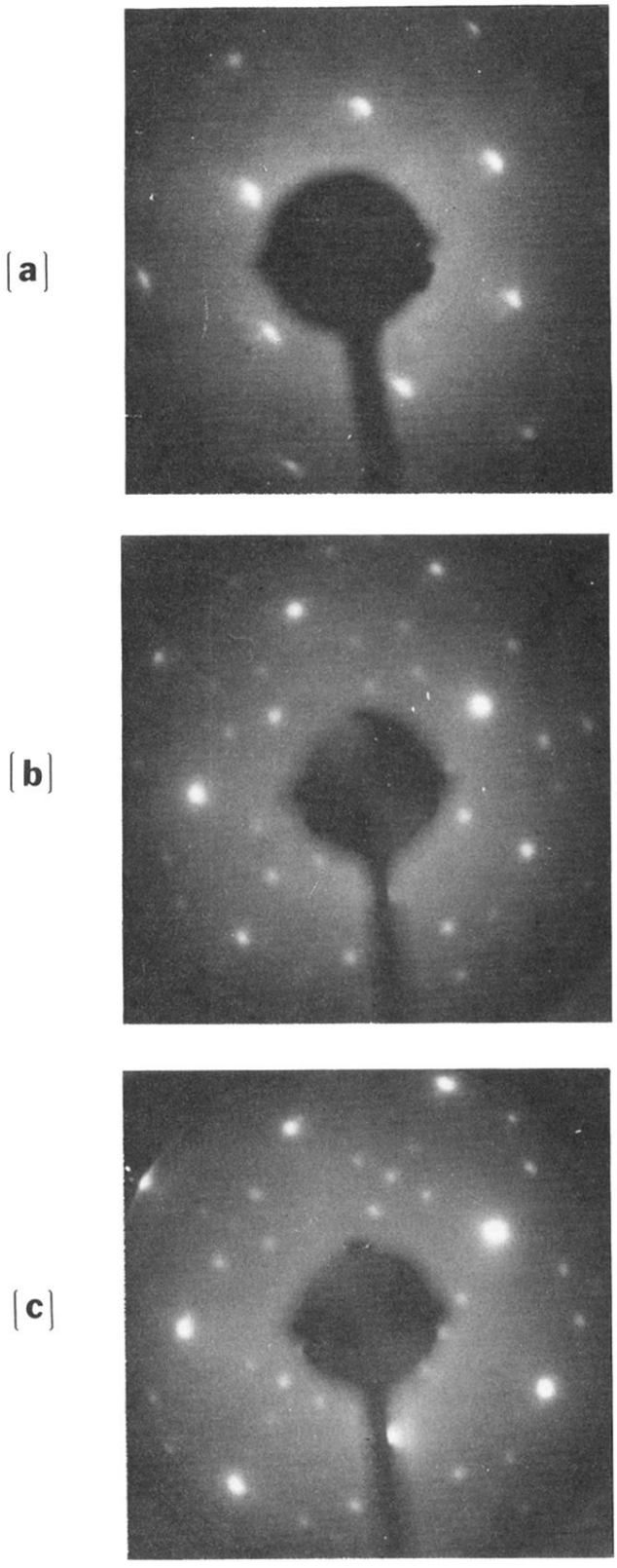

FIG. 3. (a) (1×1) hexagonal LEED pattern ($E_b = 35$ eV) for the $Cu_2O(111)$ surface following ion bombardment and annealing to 1000 K. (b) $(3\sqrt{2}\times\sqrt{2})R45°$ LEED periodicity ($E_b = 35$ eV) for the $Cu_2O(100)$ surface following ion bombardment and annealing to 800 K. (c) $(3\sqrt{2}\times\sqrt{2})(\sqrt{2}\times\sqrt{2})R45°$ pattern ($E_b = 40$ ev) formed by annealing the surface in (b) to 1000 K.

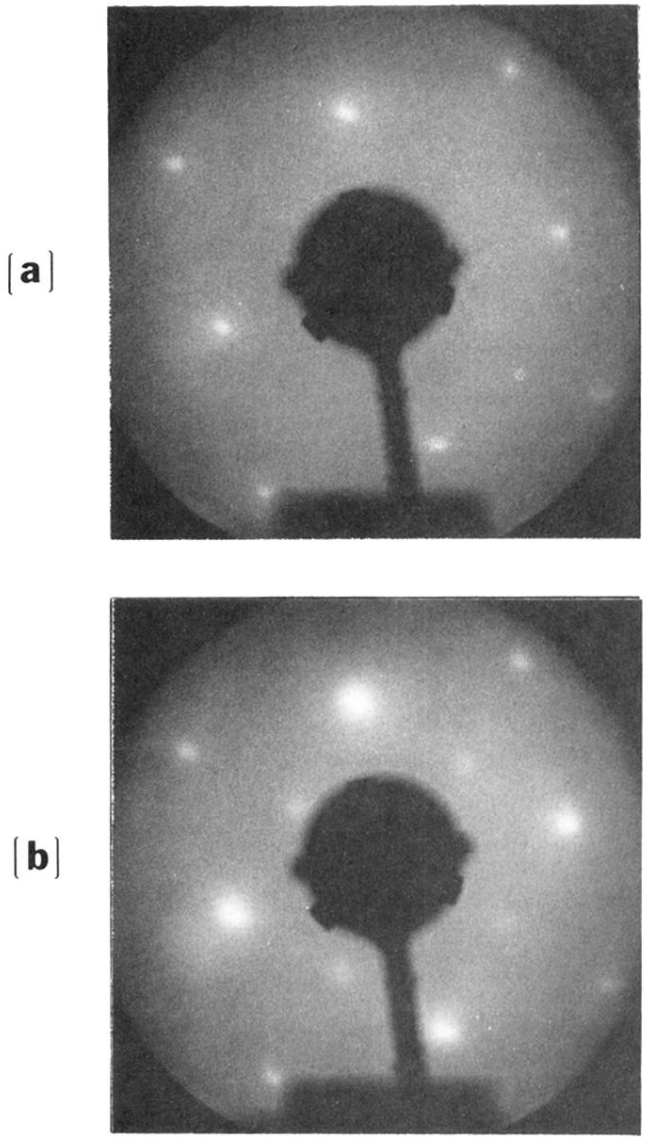

FIG. 6. (a) Square (1×1) pattern observed following 10^9-L oxygen dose on an ordered $Cu_2O(100)$ surface. (b) $(\sqrt{2}\times\sqrt{2})R45°$ periodicity observed following annealing of the surface in (a) to 400–450 K. All beam energies were 40 eV.